



AGU Books

Calcium isotope constraints on recycled carbonates in subduction-related magmas

Journal:	<i>AGU Books</i>
Manuscript ID	2019-Sep-CH-1170.R2
Wiley - Manuscript type:	Chapter
Date Submitted by the Author:	n/a
Complete List of Authors:	Simon, Justin; NASA Johnson Space Center
Primary Index Term:	1031 - Subduction zone processes (3060 , 3613 , 8170 , 8413) < 1000 - GEOCHEMISTRY
Index Term 1:	454 - Isotopic composition and chemistry (1041 , 4870) < 400 - BIOGEOSCIENCES
Index Term 2:	1038 - Mantle processes (3621) < 1000 - GEOCHEMISTRY
Index Term 3:	330 - Geochemical cycles (1030) < 300 - ATMOSPHERIC COMPOSITION AND STRUCTURE
Index Term 4:	1041 - Stable isotope geochemistry (0454 , 4870) < 1000 - GEOCHEMISTRY
Keywords:	Ca isotopes, mass-fractionation, subduction zone, mantle geochemistry, marine carbonate, carbonatite
Abstract:	<p>Calcium isotope ratios are readily mass-fractionated by low-temperature depositional processes that can be recorded in sedimentary rocks and, therefore, have the potential to track distinct geochemical signatures of recycled materials in mantle-derived igneous rocks. In this study, I report calcium isotopic compositions for well-characterized lavas from the Central American volcanic arc that exhibit a range of trace element and radiogenic isotope signatures that have been used to indicate variable amounts of subducted marine carbonate and hemipelagic sedimentary rocks, fresh carbonatite lavas from Oldoinyo Lengai Volcano, Tanzania, and an intrusive carbonatite clast erupted 12.8 ka from the Laacher See Volcano, Germany. I observed no calcium isotope evidence for recycled sedimentary rocks in the Central American arc magmas or in the Oldoinyo Lengai carbonatite volcanic rocks. They all exhibit isotopic compositions similar to rocks dominated by a primitive, mantle-like, bulk silicate Earth (BSE) composition. The exception in this work is the calcium isotope composition measured in the intrusive Laacher See carbonatite that is resolvable from BSE ($\delta^{44}\text{Ca} = 0.0$). Although this calcium isotopic signature might be related to ancient carbonate recycling, the magnitude and relatively light calcium isotopic composition ($\delta^{44}\text{Ca} = -0.4$) of this carbonatite could also reflect an origin that involved partial melting of altered lithospheric mantle from</p>

	<p>which isotopically heavy Ca-bearing fluids have been lost. The decoupled signatures between trace elements and their radiogenic isotopes and those recorded by calcium isotope data are important because they likely reflect different sources and processes, and demonstrate that sediment subduction is not a bulk mixing process.</p>

SCHOLARONE™
Manuscripts

1 **Calcium isotope constraints on recycled carbonates in subduction-related magmas**

2

3 **Author:** Justin I. Simon

4 **Affiliation:** Center for Isotope Cosmochemistry and Geochronology, Astromaterials Research &
5 Exploration Science, NASA Johnson Space Center, Houston, USA.

6 E-mail address: Justin.I.Simon@NASA.gov

7

8 **Abstract**

9 Calcium isotope ratios are readily mass-fractionated by low-temperature depositional processes
10 that can be recorded in sedimentary rocks and, therefore, have the potential to track distinct
11 geochemical signatures of recycled materials in mantle-derived igneous rocks. In this study, I
12 report calcium isotopic compositions for well-characterized lavas from the Central American
13 volcanic arc that exhibit a range of trace element and radiogenic isotope signatures that have been
14 used to indicate variable amounts of subducted marine carbonate and hemipelagic sedimentary
15 rocks, fresh carbonatite lavas from Oldoinyo Lengai Volcano, Tanzania, and an intrusive
16 carbonatite clast erupted 12.8 ka from the Laacher See Volcano, Germany. I observed no calcium
17 isotope evidence for recycled sedimentary rocks in the Central American arc magmas or in the
18 Oldoinyo Lengai carbonatite volcanic rocks. They all exhibit isotopic compositions similar to
19 rocks dominated by a primitive, mantle-like, bulk silicate Earth (BSE) composition. The exception
20 in this work is the calcium isotope composition measured in the intrusive Laacher See carbonatite
21 that is resolvable from BSE ($\delta^{44}\text{Ca} = 0.0$). Although this calcium isotopic signature might be
22 related to ancient carbonate recycling, the magnitude and relatively light calcium isotopic
23 composition ($\delta^{44}\text{Ca} = -0.4$) of this carbonatite could also reflect an origin that involved partial
24 melting of altered lithospheric mantle from which isotopically heavy Ca-bearing fluids have been
25 lost. The decoupled signatures between trace elements and their radiogenic isotopes and those
26 recorded by calcium isotope data are important because they likely reflect different sources and
27 processes, and demonstrate that sediment subduction is not a bulk mixing process.

28

29 **Introduction**

30

31 Understanding the fluxes of carbonate sediment between subducting plates and the overlying
32 mantle wedge and magmatic arc is important because sediment fluxes control mantle heterogeneity

33 and influence the global carbon cycle. In particular, when large amounts of CO₂ (as carbonate) are
34 subducted, they affect Earth's climate (DePaolo, 2004). In this study, I use calcium isotopes to
35 track recycled carbonates in subduction-related magmas because the global calcium and carbon
36 cycles are linked through carbonate formation.

37
38 Traditionally, insights into the differentiation history of the mantle come from radiogenic isotope
39 measurements of oceanic basalts, e.g., DePaolo and Wasserburg (1977), Lassiter et al. (1996), and
40 Stille et al. (1983). These observations can be used to study the origin and evolution of
41 compositionally distinct mantle reservoirs. Subduction processes play an important role in the
42 differentiation of the mantle as they can transport distinct materials into Earth's interior. In fact,
43 geochemical and isotopic systems (e.g., Sr, Nd, Pb) have been used to suggest that subducted
44 marine sediments are important to the petrogenesis of ocean island basalts, even when far from
45 any existing plate margin, e.g., Blichert-Toft et al. (1999), Cabral et al. (2013), Castillo et al.
46 (2018), and Huang and Frey (2005). Accurate interpretation of these mantle signatures is
47 complicated by the fact that both changes in source composition and time can lead to isotopic
48 heterogeneity.

49
50 Mass-dependent stable isotope compositions complement radiogenic isotope signatures because
51 they are not affected by age. Calcium isotope measurements of primitive igneous rocks have the
52 potential to provide a powerful tool to test ideas about the various possible sources of mantle
53 heterogeneity. This is because both radiogenic and stable calcium isotopes can be measured, e.g.,
54 DePaolo (2004), Huang et al. (2010; 2011), Simon and DePaolo (2010), and Simon et al. (2009).
55 Furthermore, significant stable mass-dependent calcium isotope variability is not expected to
56 originate at mantle solidus temperatures under which oceanic basalts have been generated (>1200-
57 1500°C), e.g., Putrika (2005). This is understood implicitly by the growing number of studies
58 based on mantle-derived rocks that exhibit a similar calcium isotopic composition, e.g., Amini et
59 al. (2009), Amsellem et al. (2019), Antonelli and Simon (2020), Chen et al. (2019a,b), DePaolo
60 (2004), Huang et al. (2010; 2011), Jochum et al. (2006), Kang et al. (2017), Simon and DePaolo
61 (2010), and Wombacher et al. (2009).

62

63 Subduction and recycling of sediments, in particular marine carbonates, could introduce distinctive
64 calcium isotopic variations within the mantle because marine carbonates generally have lower
65 values, i.e., lighter isotopic compositions than most igneous rocks by up to several per mil (De La
66 Rocha & DePaolo, 2000; DePaolo, 2004; Fantle & DePaolo, 2005; Farkas et al., 2007; Griffith et
67 al. 2008; Heuser et al., 2005; Kasemann et al., 2005; Watkins et al., 2017; Zhu & MacDougall,
68 1998). This isotopically light signature is commonly understood to reflect mass-dependent
69 biological fixation of Ca^{2+} into the carbonate sediments, which is a function of seawater
70 temperature and growth kinetics, but also depends on the calcium isotopic composition of seawater
71 that can fluctuate because of calcium input to the ocean from weathering of continental rocks and
72 ocean floor basalt (De La Rocha & DePaolo, 2000; DePaolo, 2004; Nielsen Lammers et al. 2020).
73 Relatively light calcium isotope ratios in Hawaiian basalts and some other mafic igneous rocks
74 have been attributed to crustal recycling (Banergee & Chakrabarti, 2019; Chen et al. 2018; Huang
75 et al., 2011; Kang et al., 2016, 2017; Liu et al., 2017), but the interpretation of the results is debated
76 (Ionov et al., 2019; Antonelli et al., 2019a).

77
78 In order to help evaluate the role that carbonate recycling plays for the evolution of Earth's
79 atmosphere and to explain isotopic heterogeneity in mantle-derived rocks, I have measured the
80 mass-dependent calcium isotope compositions of modern arc basalts from Central America. In
81 these lavas, more traditional geochemical signatures of carbonate sediment recycling have been
82 observed, including enrichments in large ion lithophile and fluid-mobile incompatible trace
83 elements, short-lived ^{10}Be abundances, heavy stable Li isotopes, and radiogenic isotopes (Chan et
84 al., 2002, 2006; Feigenson et al., 2004; Leeman et al., 1994; Morris et al., 1990; Nyström et al.,
85 1988; Patino et al., 2000; Sadofsky et al. 2008). Likewise, I report mass-dependent calcium isotope
86 measurements for young carbonatite magmas (Oldoinyo Lengai, Tanzania and Laacher See,
87 Germany) to further test the role that subducted sediment might have on the heterogeneity of the
88 mantle and to address the active debate as to whether such exotic carbonatite magmas originate
89 from low degree partial melting of a primitive mantle source or from recycling of carbonate-rich
90 surface material through subduction, e.g., Bell and Tiltonm (2002), and Walter et al. (2008).

91

92 **Analytical Methods and Samples**

93

94 *Double-spike thermal ionization mass spectrometry calcium isotope measurements*

95 The approach and analytical methods employed in this work are identical to those described in
96 Simon and DePaolo (2010) and analyses were made during the same period of time as this earlier
97 study. Briefly, bulk rock powders (~25 mg) were dissolved in a mixture of mineral acids and
98 combined with a ^{42}Ca - ^{48}Ca spike prior to chemical separation. Calcium was purified on cation
99 exchange columns (AG-50 W-X8). A ^{43}Ca single spike was used to determine column blanks and
100 yields, which were ~10-15 ng and ~99.5%, respectively. About 3 μg of purified calcium was
101 loaded in dilute HNO_3 onto rhenium filaments with dilute H_3PO_4 for each mass spectrometric
102 analysis. Calcium isotope ratios were measured with a Thermo-Finnigan Triton thermal ionization
103 multi-collector mass spectrometer (TIMS) at the University of California in the Center for Isotope
104 Geochemistry (Table 1). The ^{39}K , ^{40}Ca , ^{42}Ca , ^{43}Ca , ^{44}Ca , ^{48}Ca , and ^{49}Ti ion beams were measured
105 in a multi-step static cup configuration. The magnitude of mass interference from ^{40}K and ^{48}Ti was
106 monitored and found to be insignificant; no corrections for ^{40}K and ^{48}Ti were applied. The ^{42}Ca -
107 ^{48}Ca double spike method, e.g., Russell et al. (1978), was employed to correct for instrumental
108 mass-fractionation. The tracer $^{42}\text{Ca}/^{48}\text{Ca}$ ratio of 0.8364 ± 29 used in this study was determined by
109 isotopic measurements of tracer-standard mixtures, and by assuming that the $^{42}\text{Ca}/^{44}\text{Ca}$ ratio of
110 the calcium standard is 0.31221, the value obtained by Marshall and DePaolo (1982) and Russell
111 et al. (1978). Due to the higher abundances of ^{40}Ca (96.94%) and ^{44}Ca (2.09%) stable calcium
112 isotope variations are commonly reported as $\delta^{44}\text{Ca} = \left(\frac{^{44}\text{Ca}/^{40}\text{Ca}}{^{44}\text{Ca}/^{40}\text{Ca}}_{\text{sample}} / \left(\frac{^{44}\text{Ca}/^{40}\text{Ca}}{^{44}\text{Ca}/^{40}\text{Ca}}_{\text{standard}} - 1 \right) \right) \cdot 1000$,
113 where it is important to note that the most abundant isotope, ^{40}Ca , can also be produced by the
114 radioactive decay of ^{40}K (half-life of ~1.25 Ga). This is typically not a concern for young mafic
115 rocks, but in old rocks, stable calcium isotope variations ($\delta^{44}\text{Ca}$) must be corrected for potential
116 radiogenic ingrowth of ^{40}Ca .

117

118 More than four different reference materials are currently used to define $\delta^{44}\text{Ca}$ (see inter-
119 conversions in Antonelli and Simon, 2020). These are igneous samples that represent BSE, e.g.,
120 unmetamorphosed peridotites, komatiites, and basaltic rocks from Earth and other terrestrial
121 planets, carbonate standard SRM915a, synthetic carbonate standard SRM915b, and modern
122 seawater. In this study, reported values assume BSE=0.0‰ (reported as deviations from
123 $^{44}\text{Ca}/^{40}\text{Ca}=0.0212094 \pm 3$ and $^{43}\text{Ca}/^{40}\text{Ca}=726.840 \pm 45$ —see Simon and DePaolo, 2010). This
124 follows the approach of DePaolo (2004). When multiple measurements were made, the values

125 listed in Table 1 are weighted means with uncertainties of 2 standard errors in the mean and are
126 corrected for age and/or intrinsic $^{44}\text{Ca}/^{40}\text{Ca}$ ratio based on measurements reported by Simon et al.
127 (2009). The reported uncertainties are typically less than the 2SD long-term reproducibility of the
128 SRM915a standard, which is ± 0.14 and $\pm 0.20\text{‰}$ for $\delta^{44}\text{Ca}$ and $\delta^{43}\text{Ca}$, respectively. Based on my
129 experience, this is the current resolution of the technique and, therefore, I focus on $\delta^{44}\text{Ca}$
130 differences that are greater than $\sim 0.15\text{‰}$. When only an individual measurement is reported I
131 assign the 2SD reproducibility of the SRM915a standard.

132
133 Measured values of SRM915a were $\delta^{44}\text{Ca} = -0.97\text{‰}$ and $\delta^{43}\text{Ca} = -0.77\text{‰}$. Correcting for their
134 intrinsic $^{44}\text{Ca}/^{40}\text{Ca}$ ratio that is slightly higher than most planetary materials (see Mills et al. 2018;
135 Simon et al. 2009), shifts the values to $\delta^{44}\text{Ca} = -0.88\text{‰}$ and $\delta^{43}\text{Ca} = -0.68\text{‰}$. All data in Table 1
136 and the electronic supplement are reported corrected to the value of SRM915a ($\delta^{44}\text{Ca} = -0.95\text{‰}$)
137 as recommended by Antonelli and Simon (2020). For reference, the measured difference between
138 the average of repeat analyses of the well-known SRM915a standard and estimates of the BSE for
139 this work ($\Delta^{44}\text{Ca}_{\text{BSE-RM915a}} = 0.97 \pm 0.07\text{‰}$, 2σ , $n=11$) is similar to the difference found elsewhere,
140 e.g., Table 2.

141
142 *Igneous samples characterized for calcium isotope composition*

143 Four Central American arc basalts were selected for this study. The recent volcanism along the
144 Central American volcanic arc results from subduction of the Cocos Plate beneath the Caribbean
145 Plate (Figure 1) and consists of two regions of magmatism, the volcanic front and back-arc
146 volcanism (Carr et al., 1990). Three of the studied arc samples come from the volcanic front and
147 one is from a back-arc volcano. From north to south the samples include: Atitlan volcano,
148 Guatemala (AT-50), back-arc Yohoa volcano, Honduras (YO1), San Cristobal volcano, Nicaragua
149 (SC2), and Telica volcano, Nicaragua (TE1). Trace elements ratios (e.g., Ba/La, Ba/Th, Sr/Nb,
150 U/Th) measured in bulk samples and in olivine-bearing melt inclusions for these samples exhibit
151 a significant amount of the geochemical variation seen both locally and regionally along the
152 volcanic arc that is thought to reflect the influence of subducted sediments (Figure 2; Patino et al.,
153 2000; Sadofsky et al. 2008). Characterization of sedimentary core sampled off the coast at Deep
154 Sea Drilling Program Site 495 indicates early carbonate deposition followed by later hemipelagic
155 deposition involving large differences in incompatible elements and element ratios (e.g., Ba/Th).

156 These differences can be used to identify sediment contribution and even possibly to distinguish
157 between carbonate deposition and hemipelagic deposition (see Figure 2). In particular, the
158 carbonate sediments are believed to provide a distinctive geochemical signature that has been used
159 to track the flux of sedimentary addition to the arc magmas (Patino et al., 2000). Bulk powders of
160 the samples were obtained from M. Carr. Their major, trace element, and isotopic compositions
161 have been reported by Bolge et al. (2009), Carr et al. (1990), Feigenson (1986), Leeman et al.
162 (1994), and Patino et al. (1997; 2000), see electronic supplement.

163
164 Two fresh carbonatite lavas, collected immediately after eruptions in 2007 and 2008, from
165 Oldoinyo Lengai volcano, Tanzania were also selected for this study. Oldoinyo Lengai is located
166 on the eastern branch of the East African Rift Valley and is the only modern extrusive carbonatite
167 locality (Figure 1). The sample from 2007 (OL lava 2007) is representative of the large volumes
168 of rare, relatively Na-rich (natro-) carbonatite lavas extruded until August 2007. The younger lava
169 (OL lava 4-7-08) was extruded at a time when Oldoinyo Lengai was erupting more silicic ashes
170 (Fischer et al., 2009). Both samples were provided to me by T. Fisher.

171
172 The final sample was a clast of intrusive carbonatite from the Laacher See volcano, Germany.
173 Laacher See volcano is located in the Late Pleistocene East Eifel Volcanic Field that is part of a
174 series of intra-plate volcanic fields in Central Europe (Figure 1). The carbonatitic ejecta clast was
175 extruded ~12.9 ka as part of the most recent episode of highly alkalic and silica-undersaturated
176 magmas (Schmitt et al., 2010; references therein). The material analyzed comes from a rounded
177 nearly 100% sövite domain (~cm in size) associated with coarse-grained calcite. The sample was
178 provided by A. Schmitt who conducted an accessory mineral uranium-series dating study to
179 address the magmatic longevity of the most recent period of subvolcanic magmatism (Schmitt et
180 al., 2010).

181 182 **Results**

183
184 All but one of the studied samples have $\delta^{44}\text{Ca}$ values that are similar to the “normal” BSE
185 composition (~0‰), Figure 3 and Table 1. Their calcium isotopic compositions are similar to the
186 compositions of clinopyroxene-rich and/or unmelted and unmetasomatized peridotites (Huang et

187 al., 2010; Kang et al., 2017; Simon & DePaolo, 2010) and well-studied oceanic and continental
188 basalts, e.g., Bermingham et al. (2018), Huang et al. (2011), Simon and DePaolo (2010), and
189 Simon et al. (2017), Table 1. Honduran sample YO-1, which has MORB-like Sr and Nd isotope
190 and LILE/HFSE trace element ratios, exhibits a $\delta^{44}\text{Ca}$ ($-0.16\pm 0.14\text{‰}$ (2σ)) that is similar to the
191 samples from Nicaragua, TE1 ($\delta^{44}\text{Ca} = -0.12\pm 0.14\text{‰}$ (2σ)) and SC2 ($\delta^{44}\text{Ca} = 0.06\pm 0.05\text{‰}$ (2σ))
192 that have the most obvious trace element and radiogenic isotope signatures for sediment
193 subduction (Figure 4; Carr et al., 1990; Patino et al., 2000). The final Central American arc sample
194 from Guatemala exhibits a similar calcium isotopic composition ($\delta^{44}\text{Ca} = -0.08\pm 0.14\text{‰}$ (2σ)).
195 Likewise, both fresh Oldoinyo Lengai carbonatites OL lava 2007 ($\delta^{44}\text{Ca} -0.13\pm 0.14\text{‰}$ (2σ)) and
196 OL Lava 4-7-08 ($\delta^{44}\text{Ca} = 0.05\pm 0.13\text{‰}$ (2σ)) have calcium isotope compositions that are similar
197 to BSE. The exception in this study is the clast of intrusive carbonatite from the Laacher See
198 volcano. The carbonatitic ejecta clast has a value that is lighter than BSE ($\delta^{44}\text{Ca} = -0.39\pm 0.14\text{‰}$
199 (2σ)).

200

201 Discussion

202

203 *Calcium isotopic record of marine carbonates*

204 Calcium isotope measurements of carbonates are generally light by up to several per mil (De La
205 Rocha & DePaolo, 2000; DePaolo, 2004; Fantle & DePaolo, 2005; Farkas et al., 2007; Griffith et
206 al., 2008; Heuser et al., 2005; Kasemann et al., 2005; Watkins et al., 2017; Zhu & MacDougall,
207 1998) when compared to unmelted/non-metasomatized peridotites (Kang et al., 2017), komatiites
208 (Amsellem et al., 2019), and most igneous rocks (e.g., Antonelli & Simon, 2020; Chen et al. 2019;
209 Schiller et al., 2016; Simon & DePaolo, 2010), as shown in Figure 3. It is possible that the marine
210 carbonate record may have evolved over time towards higher $\delta^{44}\text{Ca}$ values (Farkas et al., 2007).
211 The notion that marine carbonates had light calcium isotope in the distant past has been challenged
212 recently by Blattler and Higgins (2017), who report that, on average, Precambrian carbonates
213 ($n=505$) are indistinguishable from BSE ($\pm 0.24\text{‰}$). All carbonate sediments undergo an extended
214 diagenetic evolution after deposition. However, the effects of recrystallization involving pore
215 fluids on the calcium isotopic composition in modern carbonates are minor compared to the
216 magnitude of their light calcium isotope compositions (Fantle & DePaolo, 2005; 2007). Whether
217 Precambrian carbonates were deposited with light calcium isotope compositions and subsequently

218 modified to heavy calcium isotope compositions remains to be shown, but some modification
219 might be expected due to isotopic exchange with heavy seawater and/or relatively heavy Ca-
220 bearing fluids derived from a silicate mantle or crustal reservoir (i.e., John et al. 2012).
221 Nevertheless, detailed work of Fantle and DePaolo (2005) and Griffith et al. (2008) followed up
222 by the compilation of data from over 70 studies included in Fantle and Tipper (2014) shows that
223 over at least the last ~20-30 Ma there has been a significant difference between “lighter” carbonate
224 and “normal” silicate calcium reservoirs.

225

226 *Calcium isotopic record of mantle-derived rocks*

227 Most mantle-derived rocks and peridotites studies report calcium isotope compositions similar to
228 BSE (e.g., Amsellem et al., 2019; Ionov et al., 2019; Kang et al., 2017; Simon & DePaolo, 2010).
229 There are reports of mantle rocks including peridotites that have distinctly heavy $\delta^{44}\text{Ca}$ isotopic
230 compositions, e.g., Amini et al. (2009), Lu et al. (2019), Huang et al. (2010), and Kang et al. (2017)
231 and a few that are distinctly light, e.g., Amsellem et al. (2019) and Zhao et al. (2017). In order to
232 investigate this variability Huang et al. (2010) measured mineral separates from mantle rocks and
233 found that $\delta^{44}\text{Ca}$ in orthopyroxenes (opx) are significantly heavier than their associated
234 clinopyroxenes (cpx) by 0.36-0.75‰. The magnitude and sign of the measured differences are
235 generally consistent with first principles equilibrium inter-mineral isotope fractionation
236 calculations that fundamentally depend on calcium concentration (i.e., Ca—O bond strength) and
237 temperature (Wang et al., 2017; Antonelli et al., 2019a). In detail, calcium isotope fractionation
238 between opx and cpx ($\Delta^{44/40}\text{Ca}_{\text{opx-cpx}}$) less than ~0.26‰ and greater than ~0.60‰ is likely related,
239 at least in part, to disequilibrium calcium isotopes effects such as metasomatic metamorphism
240 (Zhao et al., 2017). Disequilibrium effects have also been reported for volcanic settings during
241 rapid crystal growth (Antonelli et al., 2019b) and between opx and cpx and with other minerals
242 during granulite facies and ultrahigh-temperature metamorphism (Antonelli et al., 2019a). In these
243 cases, calcium concentration likely plays an important role, i.e., it is lower by ~1/32 in opx as
244 compared to cpx, and may be more easily affected by isotope fractionation governed by diffusive
245 loss (or gain) of calcium. This would explain why cpx tends to have compositions closer to BSE
246 but why opx compositions can vary wildly—opx as high as $\delta^{44}\text{Ca}$ ~6 has been found in mafic
247 granulite samples (Antonelli et al. 2019a). Interestingly, a recent investigation using calcium
248 isotope signatures of carbonatite and silicate metasomatism and melt percolation found little

249 evidence for calcium isotopic heterogeneity and concluded that metasomatism tends to decrease
250 $\delta^{44}\text{Ca}$ values of metasomatized mantle materials, but that its effects are usually limited ($\leq 0.3\%$)
251 (Ionov et al., 2019).

252
253 *Calcium isotopes exhibit no evidence for carbonate sediment recycling at subduction zones*

254 In the studied Central American arc magmas, I found no evidence for calcium isotopic
255 heterogeneity and thus no evidence for carbonate recycling or any isotopic fractionation related to
256 subduction. This is the case despite the fact that I selected rocks that have both little to no
257 geochemical evidence for sediment subduction, i.e., YO1 has MORB-like trace element signatures
258 and depleted mantle (DM) radiogenic isotope compositions, and rocks with strong trace element
259 and radiogenic isotope signatures for carbonate sediment subduction (Figure 2).

260
261 To date, resolvable radiogenic calcium isotopic signatures have not been observed in any oceanic
262 or arc basalts (Huang et al., 2011; Marshall & DePaolo, 1989; Simon et al., 2009). This might not
263 be surprising given the work of Caro et al. (2010) who, despite finding well-defined excesses of
264 ^{40}Ca in some river waters draining into the ocean, report that no discernable effects of ^{40}K decay,
265 to within their reported analytical precision (~ 0.4 epsilon units, 2σ), exist in marine carbonate
266 samples ranging in age from Archean to recent.

267
268 There have been recent studies of mantle-derived rocks that find little evidence that recycling of
269 carbonates affects the calcium isotope values of the mantle on a global or regional scale (Ionov et
270 al., 2019; Antonelli et al. 2019a). However, other calcium isotope studies of primitive igneous
271 rocks report evidence for recycling, e.g., Banergee and Chakrabarti (2019), Chen et al. (2018),
272 Huang et al. (2011), Kang et al. (2016, 2017), and Liu et al. (2017). My results are significant since
273 the trace element and radiogenic isotope signatures (e.g., high Ba/La, Ba/Th, $^{87}\text{Sr}/^{86}\text{Sr}$, $^{206}\text{Pb}/^{204}\text{Pb}$,
274 see Figs. 2 & 4) of Central American lavas suggest a significant contribution from subducted
275 carbonates (Patino et al., 2000; Sadofsky et al., 2008). The geochemical decoupling reported herein
276 contrasts with the signatures reported for the ocean island basalts studied by Huang et al. (2011).
277 In the Huang et al. (2011) study, stable mass-dependent calcium isotope signatures vary and
278 correlate with other geochemical parameters (i.e., Sr/Nb and $^{87}\text{Sr}/^{86}\text{Sr}$) used to support the
279 interpretation that Hawaiian lavas represent recycling of ancient calcium bearing surface materials.

280

281 All samples from the volcanic front (VF) are interpreted to be elevated in their Pb and Sr radiogenic
282 isotopes above values for back-arc lavas (BA) by the addition of a sedimentary subducted
283 component (see Figure 4; Carr et al., 1990; Feigenson & Carr, 1986; Feigenson et al., 2004; Patino
284 et al. 1997, 2000). Back-arc lavas including YO1 remain within the mantle field, reflecting
285 mixtures of MORB-like depleted mantle (DM) and enriched mantle (HIMU). The potential
286 sedimentary contribution to the arc magmas is believed to be uniform from Guatemala through
287 northern Costa Rica and the sedimentary sequence has been well-documented by the Deep Sea
288 Drilling Program (DSDP), see Patino et al. (2000). The lower section of the sedimentary sequence
289 consists of middle-lower Miocene chalky carbonate ooze and mangiferous chalk and chert that
290 are on average ~50 wt. % CaO (von Huene et al., 1982).

291

292 Subducted carbonate sediments along the Central American trough have compositions (Ba/La_{avg}
293 = 244, $Sr/Nb_{avg} = 3418$, $^{87}Sr/^{86}Sr_{avg} = 0.7086$) that can produce a distinct signature in the arc basalts
294 (Patino et al., 2000; Sadofsky et al. 2008). The calcium isotopic composition of this sediment has
295 not been measured, but modern carbonate ooze (DSDP 590B) has a $\delta^{44}Ca = -0.36 \pm 0.15\%$ (2σ)
296 (Fantle & DePaolo, 2005), similar to the modern riverine inputs to the oceans (DePaolo, 2004),
297 see Figure 3. The calcium isotope homogeneity among the studied arc magmas is particularly
298 notable when one considers the fact that they exhibit a large range in their sediment contribution
299 signatures. They exhibit compositions that range from non-existent levels typical of MORB up to
300 those near BSE in these sediment signatures (e.g., Ba/La varies from ~4 to 117, Figure 2, Sr/Nb
301 varies from 16-328, and $^{87}Sr/^{86}Sr$ varies from 0.7029-0.7041, Figure 4) as compared to the more
302 limited range recorded by the Hawaiian tholeiites ($Sr/Nb = 25-55$, $^{87}Sr/^{86}Sr = 0.7035-0.7042$),
303 considered by Huang et al. (2011) to reflect ancient carbonate recycling. These observations imply
304 that some traditional geochemical signatures for carbonate sediment subduction in arc magmas are
305 at odds with their calcium isotopic signatures.

306

307 There are several ways to explain the decoupling of the calcium isotopes and the more traditional
308 geochemical carbonate sediment signatures. First, the calcium isotope compositions of the
309 subducted carbonates could have had little mass-fractionated calcium (i.e., Farkas et al., 2007;
310 Blattler & Higgins, 2017) or their original light calcium isotopic signatures could have been

311 modified, perhaps during diagenesis, prior to subduction and therefore have had limited effect on
312 the calcium isotope composition of the studied arc magmas. I rule this out because it is unlikely
313 that modern (≤ 35 Ma) subducted carbonate sediments had BSE-like calcium isotope
314 compositions, as shown by the work of Fantle and Tipper (2014; references therein). Likewise,
315 even while the enhanced reaction in young carbonates increases the diagenetic effects, and
316 therefore their $\delta^{44}\text{Ca}$, the maximum effect ($<0.15\%$) of diagenesis is not large enough to erase the
317 $\geq 0.3\%$ light isotope effects typical of the carbonates, see Fantle and DePaolo (2007).

318
319 Second, it is possible that the flux of subducted sediment to the arc, and in particular marine
320 carbonate, is overestimated. Despite the large volumes (100's m thick) of carbonate inferred from
321 the DSDP drill cores from the subducting sediment sequence along the volcanic front, it is
322 unknown how much sediment-derived calcium is hybridized within the source reservoir(s) of the
323 arc magmas. On average CaO is 4-5x more enriched in the carbonate sediment than the arc
324 magmas. MORB-like magmas have CaO contents that are the same or slightly higher than
325 comparable primitive arc basalts (Patino et al. 1997; Presnall & Hoover, 1987). So, unlike Pb, Sr,
326 and Nd that are found in relatively low abundances in the mantle, and therefore must come from a
327 subducted component, perhaps sediments, to explain the elevated abundances in the arc basalts,
328 all of the CaO needed in the arc basalts can be potentially provided by the mantle. For the most
329 part these trace elements also behave incompatibly and will preferentially contribute, along with
330 H_2O and other fluid mobile LILE, to the arc flux. In contrast, calcium acts compatibly. Therefore,
331 any process that creates new Ca-bearing phases, such as the "reaction pyroxenite" described by
332 Straub et al. (2008; 2011), would effectively trap sediment-derived Ca. As this material sinks into
333 the mantle, this may help explain why some or most subducted carbonate calcium is added to long,
334 deep mantle convection cycles contributing to the formation of ocean island basalts as suggested
335 by Huang et al. (2011) (and possibly the carbonatites discussed in the following section), rather
336 than the arc.

337
338 Third, the calcium isotope signatures may reflect a scenario in which the light calcium isotopic
339 signatures of the subducted sediment are diluted by mixture with relatively heavy calcium
340 reservoir(s), i.e., seawater and/or crustal rocks with BSE calcium isotopic compositions. Clear
341 evidence of sediment subduction in the Central American arc is complicated by the fact that the

342 radiogenic isotope compositions of the subducted sediments are relatively unradiogenic for marine
343 sediments (cf. Feigenson et al., 2004). The exception may be Guatemalan lava AT-50, but notably
344 its Nd-Sr isotopes could also reflect addition of crust and not necessarily subducted sediment
345 (Figure 4). Some of the trace element variability used as evidence for subducted sediment (Ba/Th)
346 could also be explained by the mobilization of Ba over Th in fluids derived from subducted altered
347 oceanic crust (Figure 4) as seen in oceanic island arc basalts (Turner et al., 1996; Hawkesworth et
348 al., 1997). Moreover, calcium mobilized in fluids extracted via deserpentinization reactions, as
349 subducted rocks rise in temperature and pressure, might buffer the light carbonate signatures. It
350 has been reported that subducted fluids could evolve isotopically during transport and fluid-rock
351 interaction, becoming enriched in heavy isotopes as they rise through the slab into the subvolcanic
352 arc (John et al., 2012). It follows that mixing with isotopically heavy altered oceanic crust could
353 offset the effects of the calcium from carbonate sediment which is isotopically light and produce
354 BSE calcium isotope compositions for the arc lavas.

355

356 *Mantle source(s) of calcium in carbonatite magmas*

357 The similar $\delta^{44}\text{Ca}$ of the studied Oldoinyo Lengai carbonatite lavas and terrestrial basalts (i.e.,
358 BSE composition) suggests a mantle-source for their calcium. This interpretation is consistent with
359 the general consensus that carbonatites originate from low-degrees of partial melting of the mantle
360 (see Bell & Tilton, 2002; Walter et al., 2008). It is also consistent with studies that conclude
361 carbonatite volcanoes extrude primordial volatiles (CO_2 , He, N_2 and Ar) that are indistinguishable
362 from those emitted along mid-ocean ridges despite the fact that Oldoinyo Lengai carbonatites
363 occur in a setting far removed from oceanic spreading centers (Fisher et al. 2009). It is possible
364 that Oldoinyo Lengai lavas, which are natrocarbonatite, are not representative of more Ca-rich
365 carbonatite magmas. Extruded carbonatites, being composed largely of soluble carbonates, are
366 easily weathered and therefore unlikely to be preserved in the geological record. The question of
367 why this volcano extrudes lavas that are chemically different to older carbonatite centers, and
368 whether ancient carbonatites were all originally natrocarbonatites and subsequently altered to
369 calciocarbonatites remains unanswered (Dawson et al., 1987; Zaitsev & Keller, 2006).

370

371 *Origin of the light calcium isotope composition of Laacher See and other intrusive carbonatites*

372 The distinctly light calcium isotope signature ($\delta^{44}\text{Ca} = -0.39 \pm 0.14\text{‰}$ (2σ)) of the intrusive Laacher
373 See carbonatite is the sole outlier in this study, and is distinct from what is found in most igneous
374 samples (see compilations in Antonelli & Simon, 2020; Schiller et al., 2016). It is possible that the
375 mass-dependent calcium isotopic deficit seen in Laacher See carbonatite is an artifact produced by
376 relatively large (~ 4 epsilon-unit) radiogenic ^{40}Ca effects, as can be seen in Precambrian samples
377 (e.g., Antonelli et al., 2019c; Mills et al., 2018; Simon et al., 2009). This is unlikely given the fact
378 that the carbonatite clast studied was cogenetic with its ~ 12.9 ka phonolite host, which exhibits
379 negligible evidence for assimilation, and contained zircons that range from 32.6 ± 4.1 ka to near-
380 eruption in age (Schmitt et al., 2010).

381
382 The calcium isotope composition of the Laacher See carbonatite could originate from recycling of
383 isotopically light marine carbonate as suggested recently for other carbonatites (Amsellem et al.,
384 2020). This would involve carbonate subduction through a long deep convection cycle, which is
385 required given the fact that the East Eifel Volcanic Field is in Central Europe far from a modern
386 subduction zone. Amsellem et al. (2020) recently reported light calcium isotope data for a large
387 number of Ca-, Mg-, and Fe-rich carbonatites spanning from ~ 3 Ga to ~ 1 Ma (Amsellem et al.,
388 2020). Their findings are important because they may provide timing constraints for the onset of
389 plate tectonics and subduction of marine sediments. Furthermore, their conclusions imply that
390 since at least 3 Ga there has been relatively similar levels of marine biomineralization, seawater
391 conditions, and continental weathering to produce isotopically light marine carbonate. This does
392 not appear to be true, however, as over approximately the same timespan (~ 3.0 to 0.7 Ga) there is
393 little evidence for isotopically light marine carbonate in the geologic record (Blatter & Higgins,
394 2017). In fact, the extensive Precambrian carbonate record reported by Blatter and Higgins (2017)
395 is dominated by BSE calcium isotope compositions. This record poses a serious problem for the
396 interpretations of Amsellem et al. (2020), which necessitate that ancient carbonatites form from
397 recycled light marine carbonates.

398
399 The Laacher See carbonatite is notable, in part, because it is the youngest intrusive carbonatite
400 example known on Earth. It may also be important that it is an intrusive rather than an extruded
401 sample. Another significant characteristic of the Laacher See carbonatite is that its oxygen isotopic
402 composition is similar to the relatively narrow range ($\delta^{18}\text{O}_{\text{SMOW}} = 5\text{-}8\text{‰}$) exhibited by mantle-

403 derived mafic rocks (Schmitt et al. 2010; Taylor et al., 1967). In general, more silicic igneous rocks
404 and most metamorphic and sedimentary rocks exhibit higher $\delta^{18}\text{O}$ values. This similarity has been
405 used to suggest a possible genetic relationship between the Laacher See carbonatites and rocks that
406 are commonly believed to originate in the lower crust or upper mantle. Because oxygen is a major
407 component of the studied materials, their oxygen isotopic composition has been used to argue that
408 it is difficult for the Laacher See carbonatites to have formed by addition of any significant
409 sedimentary carbonate component, which generally have much higher oxygen isotope
410 compositions ($\delta^{18}\text{O}_{\text{SMOW}} = 15\text{-}25\text{‰}$; Taylor et al., 1967). It follows, therefore, that its CO_2 , and
411 perhaps calcium, is likely also primary and not due to marine carbonate recycling. Taylor et al.
412 (1967) do point out, however, that the Laacher See carbonatites could form from assimilation of
413 carbonate if these materials had undergone recrystallization and oxygen exchange with primary
414 igneous rocks. It should also be noted that despite the fact that a large number of carbonatite
415 complexes around the world do exhibit mantle-like C and O isotopic signatures, some exhibit much
416 heavier oxygen isotope compositions than the Laacher See carbonatites. These heavy oxygen
417 isotope values are consistent with what might be produced by assimilation of sedimentary
418 carbonate country rock (e.g., Santos and Clayton, 1995; Wei et al., 2020). Consequently, the
419 relatively constant $\delta^{44}\text{Ca} \sim -0.4$ values seen in carbonatites, over the past 3 Ga, probably reflect a
420 more universal mass-fractionation process rather than the incorporation of a relatively constant
421 amount (6-7%) of recycled marine carbonate sediment into their mantle sources (cf. Amsellem et
422 al., 2020).

423
424 Laacher See carbonatite has had a protracted sub-solidus history as an intrusive rock and has a
425 calcium isotopic composition that is similar in magnitude and sign to the mass-fractionation seen
426 for carbonatite metasomatism (Ionov et al. 2019). Therefore, the most likely explanation for its
427 calcium isotopic composition is that its formation included fluid-alteration and/or a partially
428 dehydrated source rock from which isotopically heavy Ca-bearing fluids have been lost, analogous
429 to that reported by John et al. (2012) for metasomatism in subduction zones. Given that a majority
430 of carbonatites have a similar light calcium isotopic composition, and yet marine carbonates may
431 not have had isotopically light calcium isotope compositions in the past, there is no simple scenario
432 in which marine carbonate recycling is the dominate explanation for their calcium isotopic
433 composition.

434

435 **Conclusions**

436

437 Studied Central American arc magmas have no calcium isotope evidence for carbonate recycling.
438 This is observed even for magmas with strong trace element and radiogenic isotope signatures
439 indicating sediment subduction. The decoupled signatures are important because they likely reflect
440 different sources and processes, and demonstrate that sediment subduction is not a bulk mixing
441 process. Fresh Oldoinyo Lengai carbonatites also have $\delta^{44}\text{Ca}$ values that are similar to unmelted
442 peridotites, komatiites, and most basalts, which again implies a primitive mantle-derived calcium
443 source. The possible exception comes from the intrusive Laacher See carbonatite. Its calcium
444 isotopic signature could be related to carbonate sediment recycling in a long deep convective cycle.
445 Alternatively, the relatively light calcium isotopic composition ($\delta^{44}\text{Ca} = -0.39$) measured in the
446 Laacher See carbonatite, and recently found in other carbonatites, may be associated with a process
447 in which an isotopically heavy Ca-bearing fluid was extracted during dehydration of its
448 lithospheric mantle source, mass-fractionating its original BSE calcium isotopic composition.

449

450 **Acknowledgments**

451 The author would like to thank Don DePaolo for his friendship, support, and tutelage. Being a part
452 of the Earth and Planetary Science Department at University of California at Berkeley and in
453 particular a member of the Center for Isotope Geochemistry was a highlight of my career. I have
454 learned a great deal from discussions and collaborations with past and present members of the CIG
455 group. The editorial handling by Ken Sims and helpful constructive reviews by Michael Antonelli
456 and two anonymous reviewers are much appreciated. Michael Carr, Tobias Fisher, and Axel
457 Schmitt are thanked for generously providing sample material. This work was supported by NSF
458 Petrology and Geochemistry and NASA Astrobiology programs (that partly supported my
459 postdoctoral research with Don DePaolo while at the University California at Berkeley) and NASA
460 Planetary Science funding.

461

462 Table 1. Mass-dependent calcium isotope compositions of igneous rocks and standards.

463

464 Table 2. Difference between igneous rocks used to estimate $\delta^{44}\text{Ca}$ of BSE and SRM915a standard
465 for various research laboratories.

466
467 Figure 1. Maps of Central America, Eastern Africa, and Europe showing location of the studied
468 samples. The location of the DSDP Site 495, off the coast of Guatemala, is also indicated (Central
469 American map modified from Patino et al. 2000).

470
471 Figure 2. Regional variations in trace element ratios along the Central American volcanic arc.
472 MORB-like Ba/La and Ba/Th values occur in Honduras volcanoes whereas maximum values,
473 believed to be tracers of hemipelagic sediment and marine carbonate, respectfully, occur in western
474 Nicaraguan volcanoes (data from Patino et al., 1997; 2000).

475
476 Figure 3. Calcium isotopic composition of Central American volcanic arc magmas (this study),
477 extrusive Oldoinyo Lengai carbonatite lavas (this study), and intrusive Laacher See carbonatite
478 clast (this study). Values for unmelted/unmetamorphosed peridotites, komatiites, terrestrial
479 basalts, seawater, marine carbonates, SRM915a carbonate, and the effect of metasomatism shown
480 for reference (Antonelli et al. 2019a; Amsellem et al., 2019; Bermingham et al., 2018; Fantle &
481 DePaolo, 2005; Huang et al., 2010, 2011; Ionov et al., 2019; Kang et al., 2017; Simon & DePaolo,
482 2010; Simon et al., 2017). Not shown are the Precambrian carbonate data of Blattler and Higgins
483 (2017) that exhibit an average $\delta^{44}\text{Ca}$ that is indistinguishable from BSE calcium isotope
484 composition.

485
486 Figure 4. Ba/Th- $^{87}\text{Sr}/^{86}\text{Sr}$ (a), $^{143}\text{Nd}/^{144}\text{Nd}$ - $^{87}\text{Sr}/^{86}\text{Sr}$ (b), and $^{206}\text{Pb}/^{204}\text{Pb}$ - $^{87}\text{Sr}/^{86}\text{Sr}$ (c) diagrams for
487 Central American volcanic arc lavas. All samples from the volcanic front (VF) have geochemical
488 signatures interpreted to be elevated above values for back-arc lavas (BA) by the addition of a
489 sedimentary subducted component, e.g., enriched in $^{87}\text{Sr}/^{86}\text{Sr}$. Back-arc lavas including YO1
490 remain within the mantle field, reflecting mixtures of MORB-like depleted mantle and HIMU,
491 enriched mantle (data and illustrative mixing curves from Carr et al., 1990; Feigenson & Carr,
492 1986; Feigenson et al., 2004; Patino et al. 1997; 2000). Orange and gray squares represent
493 hemipelagic and carbonate DSDP 495 sediment compositions, respectively.

494

495 **References**

- 496 Antonelli, M.A., Schiller, M., Schauble, E.A., Mittal, T., DePaolo, D.J., Chacko, T., Grew, E.S.,
497 Tripoli, B. (2019a) Kinetic and equilibrium Ca isotope effects in high-T rocks and
498 minerals. *Earth and Planetary Science Letters*, 517, 71–82.
- 499 Antonelli, M.A., Mittal, T., McCarthy, A., Tripoli, B., Watkins, J.M., DePaolo, D.J. (2019b) Ca
500 isotopes record rapid crystal growth in volcanic and subvolcanic systems. *Proceedings of*
501 *the National Academy of Sciences*, 116, 20315-20321.
- 502 Antonelli, M.A., DePaolo, D.J., Chacko, T., Grew, E.S., Rubatto, D. (2019c) Radiogenic Ca
503 isotopes confirm post-formation K depletion of lower crust. *Geochemical Perspectives*
504 *Letters*, 9, 43-48.
- 505 Antonelli, M.A., Simon, J.I. (2020) Calcium isotopes in high-temperature terrestrial processes.
506 *Chemical Geology*, 548, 119651, ISSN 0009-2541.
- 507 Amini, M., Eisenhauer, A., Bohm, F., Holmden, C., Kreissing, K., Hauff, F., & Jochum, K.P.
508 (2009). Calcium isotopes ($\delta^{44}/^{40}\text{Ca}$) in MPI-DING reference glasses, USGS rock powders
509 and various rocks: Evidence for Ca isotope fractionation in terrestrial silicates.
510 *Geostandards and Geoanalytical Research*, 33, 231-247.
- 511 Amsellem, E., Moynier, F., & Puchtel, I. S. (2019). Evolution of the Ca isotopic composition of
512 the mantle. *Geochimica et Cosmochimica Acta*, 258, 195-206.
- 513 Amsellem, E., Moynier, F., Bertrand, H., Bouyon, Am., Mata, J., Tappe, S., Day, J. M. D. (2020)
514 Calcium isotopic evidence for the mantle sources of carbonatites. *Science Advances*, 6,
515 eaba3269, DOI: 10.1126/sciadv.aba3269.
- 516 Banerjee, A., Chakrabarti, R. (2019) A geochemical and Nd, Sr and stable Ca isotopic study of
517 carbonatites and associated silicate rocks from the ~65 Ma old Ambadongar carbonatite
518 complex and the Phenai Mata igneous complex, Gujarat, India. *Lithos*, 326-327, 572-585.
- 519 Bell, K., & Tilton, G.R. (2002). Probing the mantle: The story from carbonatites. *EOS*,
520 *Transactions American Geophysical Union*, 83, 273-277.
- 521 Bermingham, K. R., Gussone, N., Mezger, K., & Krause, J. (2018). Origins of mass-dependent
522 and mass-independent Ca isotope variations in meteoritic components and meteorites.
523 *Geochimica et Cosmochimica Acta*, 226, 206-223.
- 524 Blattler, C. L., & Higgins, J. A. (2017). Testing Urey's carbonate-silicate cycle using the calcium
525 isotopic composition of sedimentary carbonates. *Earth and Planetary Science Letters*, 479,
526 241-251.
- 527 Blichert-Toft, J., Frey, F. A., & Albarede, F. (1999). Hf isotope evidence for pelagic sediments in
528 the source of Hawaiian basalts. *Science*, 285, 879-882.
- 529 Bolge, L.L., Carr, M.J., Milidakis, K.K., Lindsay, F.N., Feigenson, M.D. (2009) Correlating
530 geochemistry, tectonics, and volcanic volume along the Central American volcanic front.
531 *Geochemistry, Geophysics, Geosystems*, 10, 1-15.
- 532 Cabral, R.A., Jackson, M.G., Rose-Koga, E.F., Koga, K.T., Whitehouse, M.J., Antonelli, M.A.,
533 Farquhar, J., Day, J.M.D., Hauri, E.H. (2013) Anomalous sulphur isotopes in plume lavas
534 reveal deep mantle storage of Archean crust. *Nature*, 496, 490-493.
- 535 Caro, G., Papanastassiou, D. A., & Wasserburg, G. J. (2010). ^{40}K - ^{40}Ca isotopic constraints on
536 the oceanic calcium cycle. *Earth and Planetary Science Letters*, 296, 124-132.
- 537 Carr, M. J., Feigenson, M. D., & Bennett, E. A. (1990). Incompatible element and isotopic
538 evidence for tectonic control of source mixing and melt extraction along the Central
539 American Arc. *Contributions to Mineralogy and Petrology*, 105, 369-380.

- 540 Castillo, P. R., Maclsaac, C., Perry, S., & Veizer, J. (2018). Marine Carbonates in the Mantle
541 Source of Oceanic Basalts: Pb Isotopic Constraints. *Scientific Reports, Vol. 8* (Article
542 number: 14932).
- 543 Chan, L.-H., Leeman, W.P., & You, C.-F. (2002). Lithium isotopic composition of Central
544 American volcanic arc lavas: implications or modification o subarc mantle by slab-erived
545 fulids: correction. *Chemical Geology, 182* (293-300).
- 546 Chan, L.-H., Leeman, W.P., Plank, T. (2006) Lithium isotopic composition of marine sediments.
547 *Geochemistry, Geophysics, Geosystems, 7*, 1-25.
- 548 Chen, C., Ciazela, J., Li, W., Dai, W., Wang, Z., Foley, S.F., Li, M., Hu, Z., Liu, Y. (2019a)
549 Calcium isotopic compositions of oceanic crust at various spreading rates. *Geochimica et*
550 *Cosmochimica Acta, 278*, 272-288.
- 551 Chen, C., Dai, W., Wang, Z., Liu, Y., Li, M., Becker, H., Foley, S.F., 2019b. Calcium isotope
552 fractionation during magmatic processes in the upper mantle. *Geochimica et*
553 *Cosmochimica Acta, 249*, 121–137.
- 554 Chen, C., Liu, Y., Feng, L., Foley, S.F., Zhou, L., Ducea, M.N., Hu, Z. (2018) Calcium isotope
555 evidence for subduction-enriched lithospheric mantle under the northern North China
556 Craton. *Geochimica et Cosmochimica Acta, 238*, 55-67.
- 557 Dawson, J. B., Garson, M. S., & Roberts, B. (1987). Altered former alkalic carbonatite lava from
558 Oldoinyo Lengai, Tanzania, inferences for calcite carbonatite lavas. *Geology, 15*, 765-768.
- 559 De La Rocha, C. L., & DePaolo, D. J. (2000). Isotopic evidence for variations in the marine
560 calcium cycle over the cenozoic. *Science, 289* (5482), 1176-1178.
- 561 DePaolo, D. J. (2004). Calcium isotopic variations produced by biological, kinetic, radiogenic and
562 nucleosynthetic processes. *Geochemistry of Non-Traditional Stable Isotopes, 55*, 255-288.
- 563 DePaolo, D. J., & Wasserburg, G. J. (1977). The sources of island arcs as indicated by Nd and Sr
564 isotopic studies. *Geophysical Research Letters, 4*, 465-468.
- 565 Fantle, M., & DePaolo, D. J. (2005). Variations in the marine Ca cycle over the past 20 million
566 years. *Earth and Planetary Science Letters, 237*, 102-117.
- 567 Fantle, M. S., & Tipper, E. T. (2014). Calcium isotopes in the global biogeochemical Ca cycle:
568 Implications for development of a Ca isotope proxy. *Earth -Sciences Reviews, 129*, 148-
569 177.
- 570 Farkas, J., Buhl, D., Blenkinsop, J., & Veizer, J. (2007). Evolution of the oceanic calcium cycle
571 during the late Mesozoic: evidence from $\delta^{44}/^{40}\text{Ca}$ of marine skeletal carbonates. *Earth*
572 *and Planetary Science Letters, 253*(96-111).
- 573 Feigenson, M.D., Carr, M.J. (1986) Positively correlated Nd and Sr isotope ratios of lavas from
574 the Central American volcanic front. *Geology, 14*, 79-82.
- 575 Feigenson, M.D., Carr, M.J., Maharaji, S.V., Juliano, S., Bolge, L.L. (2004) Lead isotope
576 composition of Central American Volcanoes: Influence of the Galapagos Plume.
577 *Geochemistry Geophysics Geosystems, 5*, 1-14.
- 578 Fischer, T. P., Burnard, P., Marty, B., Hilton, D. R., Furi, E., Palhol, F., . . . Mangasini, F. (2009).
579 Upper-mantle volatile chemistry at Oldoinyo Lengai volcano and the origin of carbonatites.
580 *Nature, 459*, 77-80.
- 581 Griffith, E. M., Paytan, A., Caldeira, K., Bullen, T. D., & Thomas, E. (2008). A dynamic marine
582 Ca cycle during the past 28 million years. *Science, 322*, 1671-1674.
- 583 Hawkesworth, C., Turner, S., Peate, D., McDermott, F., van Calsteren, P. (1997) Elemental U and
584 Th variations in island arc rocks: implications for U-series isotopes. *Chemical Geology,*
585 *139*, 207-221.

- 586 Heuser, A., Eisenhauer, A., Bohm, F., Wallmann, K., Gussone, N., Pearson, P. N., . . . Dullo, W.
587 C. (2005). Calcium isotope ($\delta^{44}/^{40}\text{Ca}$) variations of Neogene planktonic foraminifera.
588 *Paleoceanography*, 20. doi:org/10.1029/2004PA001048
- 589 Huang, S., Farkaš, J., & Jacobsen, S. B. (2011). Stable calcium isotopic compositions of Hawaiian
590 shield lavas: Evidence for recycling of ancient marine carbonates into the mantle.
591 *Geochimica et Cosmochimica Acta*, 75, 4987-4997.
- 592 Huang, S., Frarkaš, J., & Jacobsen, S. B. (2010). Calcium isotopic fractionation between
593 clinopyroxene and orthopyroxene from mantle peridotites. *Earth and Planetary Science
594 Letters*, 292, 337-344.
- 595 Huang, S., & Frey, F. A. (2005). Recycled oceanic crust in the Hawaiian Plume: evidence from
596 temporal geochemical variations within the Koolau Shield. *Contributions to Mineralogy
597 and Petrology*, Vol 149, 556-575.
- 598 Ionov, D. A., Yu, H., Q., Kang, J.-T., Golovin, A. V., Oleinikov, O. B., Zheng, W., . . . Huang,
599 F. (2019). Calcium isotopic signatures of carbonatite and silicate metasomatism, melt
600 percolation and crustal recycling in the lithospheric mantle. *Geochimica et Cosmochimica
601 Acta*, 248, 1-13.
- 602 Jochum, K. P., Stoll, B., Herwig, K., Willbold, M., Hofmann, A. W., Amini, M., . . . Woodhead,
603 J. D. (2006). MPI-DING reference glasses for in situ microanalysis: New reference values
604 for element concentrations and isotope ratios. *Geochemistry Geophysics Geosystems*, 7.
605 doi:org/10.1029/2005GC001060
- 606 John, T., Gussone, N., Padlachikov, Y. Y., Bebout, G. E., Dohmne, R., Halama, R., . . . Seitz, H.-
607 M. (2012). Volcanic arcs fed by rapid pulsed fluid flow through subducting slabs. *Nature
608 GeoScience*, 5, 489-492.
- 609 Kang, J.-T., Ionov, D. A., Liu, F., Zhang, C.-L., Golovin, A. V., Qing, L.-P., . . . Huang, F. (2017).
610 Calcium isotopic fractionation in mantle peridotites by melting and metasomatism and Ca
611 isotope composition of the Bulk Silicate Earth. *Earth and Planetary Science Letters*, 474,
612 128-137.
- 613 Kang, J.-T., Zhu, H.L., Liu, Y.F., Liu, F., Wu, F., Hao, Y.T., Zhi, X.C., Zhang, Z.F., Huang, F.
614 (2016) Calcium isotopic composition of mantle xenoliths and minerals from Eastern China.
615 *Geochimica et Cosmochimica Acta*, 174, 335-344.
- 616 Kasemann, S. A., Hawkesworth, C. J., Prave, A. R., Fallick, A. E., & Pearson, P. N. (2005). Boron
617 and calcium isotope composition in Neoproterozoic carbonate rocks from Namibia:
618 evidence for extreme environmental change. *Earth and Planetary Science Letters*, 231, 73-
619 86.
- 620 Lassiter, J. C., DePaolo, D. J., & Tatsumoto, M. (1996). Isotopic evolution of Mauna Kea volcano:
621 Results from the initial phase of the Hawaii Scientific Drilling Project. *Journal of
622 Geophysical Research*, 101 (11769-11780).
- 623 Leeman, W. P., Carr, M. J., & Morris, J. D. (1994). Boron geochemistry of the Central American
624 Volcanic Arc: Constraints on the genesis of subduction-related magmas. *Geochimica et
625 Cosmochimica Acta*, 58, 149-168.
- 626 Lu, W.-N., Yongsheng, H. Wang, Y., and Ke, S. (2019). Behavior of calcium isotopes during
627 continental subduction recorded in meta-basaltic rocks. *Geochimica et Cosmochimica
628 Acta*, in press online.
- 629 Lui, F., Li, X., Wang, G., Liu, Y., Zhu, H., Kang, J., Huang, F., Sun, W., Xia, X., Zhang, Z. (2017).
630 Marine carbonate component in the mantle beneath the Southeastern Tibetan Plateau:

- 631 evidence from magnesium and calcium isotopes. *J. Geophys. Res. Solid Earth*, 122, 9729–
632 9744.
- 633 Marshall, B. D., & DePaolo, D. J. (1982). Precise Age-Determinations and Petrogenetic Studies
634 Using the K-Ca Method. *Geochimica et Cosmochimica Acta*, 46 (12), 2537-2545.
- 635 Marshall, B. D., & DePaolo, D. J. (1989). Calcium Isotopes in Igneous Rocks and the Origin of
636 Granite. *Geochimica et Cosmochimica Acta*, 53(4), 917-922.
- 637 Morris, J. D., Leeman, W. P., & Tera, F. (1990). The subducted component of island arc lavas;
638 constraints from Be isotopes and B-Be systematics. *Nature*, 344, 31-36.
- 639 Nielsen Lammers, L., Kulasinski, K., Zarzycki, P., DePaolo, D.J. (2020) Molecular simulations of
640 kinetic stable calcium isotope fractionation at the calcite-aqueous interface. *Chemical
641 Geology*, 532, 119315.
- 642 Nyström, J.O., Levy, B., Troëng, B., Ehrenborg, J., Carranza, G. (1988) Geochemistry of volcanic
643 rocks in a traverse through Nicaragua. *Revista Geológica de América Central*, 8, 77-109.
- 644 Patino, L.C., Carr, M.J., & Feigenson, M.D. (1997) Cross-arc geochemical variations in volcanic
645 fields in Honduras, C.A.: progressive changes in source with distance from the volcanic
646 front. *Contributions to Mineralogy and Petrology*, 129, 341-351.
- 647 Patino, L.C., Carr, M.J., & Feigenson, M.D. (2000). Local and regional variations in Central
648 American arc lavas controlled by variations in subducted sediment input. *Contributions to
649 Mineralogy and Petrology*, 138, 265-283.
- 650 Putrika, K. D. (2005). Mantle potential temperatures at Hawaii, Iceland, and the mid-ocean ridge
651 system, as inferred from olivine phenocrysts: evidence for thermally driven mantle plumes.
652 *Geochemistry Geophysics Geosystems*, 6(Q05L08). doi:10.1029/2005GC000915
- 653 Presnall, D.C., Hoover, J.D. (1987). High pressure phase equilibrium constraints on the origin of
654 mid-ocean ridge basalts, in Mysen, B.O. (Ed.), *Magmatic Processes: Physicochemical
655 Principles*, Special Publication-Geochemical Society, 1, 75-89.
- 656 Russell, W. A., Papanastassiou, D. A., & Tombrello, T. A. (1978). Ca Isotope Fractionation on
657 Earth and Other Solar-System Materials. *Geochimica et Cosmochimica Acta*, 42(8), 1075-
658 1090.
- 659 Sadofsky, S.J., Portnyagin, M., Hoernle, K., van den Bogaard, P. (2008) Subduction cycling of
660 volatiles and trace elements through the Central American volcanic arc: evidence from melt
661 inclusions. *Contributions to Mineralogy and Petrology*, 155, 433-456.
- 662 Santos, R.V., Clayton, R.N. (1995) Variations of oxygen and carbon isotopes in carbonatites: A
663 study of Brazilian alkaline complexes. *Geochimica et Cosmochimica Acta*, 59, 1339-1352.
- 664 Schmitt, A. K., Wetzel, F., Cooper, K. M., Zou, H., & Worner, G. (2010). Magmatic Longevity of
665 Laacher See Volcano Eifel, Germany) Indicated by U-Th Dating of Intrusive Carbonatites.
666 *Journal of Petrology*, 51(5), 1053-1085.
- 667 Schiller M., Gussone, N., Wombacher, F. (2016) High Temperature Geochemistry and
668 Cosmochemistry. In: Calcium Stable Isotope Geochemistry. *Advances in Isotope
669 Geochemistry*. Springer, Berlin, Heidelberg, 223-245.
- 670 Simon, J. I., & DePaolo, D. J. (2010). Stable calcium isotopic composition of meteorites and rocky
671 planets. *Earth and Planetary Science Letters*, 289, 457-466.
- 672 Simon, J. I., DePaolo, D. J., & Moynier, F. (2009). Calcium isotope composition of meteorites,
673 Earth, and Mars. *Astrophysical Journal*, 702, 707-715.
- 674 Simon, J. I., Jordan, M. K., Tappa, M. J., Schauble, E. A., Kohl, I. E., & Young, E. D. (2017).
675 Calcium and titanium isotope fractionation in refractory inclusions: Tracers of

- 676 condensation and inheritance in the early solar protoplanetary disk. *Earth and Planetary*
677 *Science Letters*, 472, 277-288.
- 678 Stille, P., Unruh, D. M., & Tatsumoto, M. (1983). Pb, Sr, Nd and Hf isotopic evidence of multiple
679 sources for Oahu, Hawaii basalt. *Nature*, 304, 25-29.
- 680 Straub, S.M., Gomez-Tuena, A., Stuart, F.M., Zellmer, G.F., Espinasa-Perena, R., Cai, Y., Iizuka,
681 Y. (2011) Formation of hybrid arc andesites beneath thick continental crust. *Earth and*
682 *Planetary Science Letters*, 303, 337-347.
- 683 Straub, S.M., LaGatta, A.B., Martin-Del Pozzo, A.L., Langmuir, C.H. (2008) Evidence for high-
684 Ni olivines for a hybridized peridotite/pyroxenite source for orogenic andesites from the
685 central Mexican Volcanic Belt. *Geochemistry, Geophysics, Geosystems*, 9, 1-33.
- 686 Turner, S., Hawkesworth, C., van Calsternen, P., Heath, E., Macdonald, R., Black, S. (1996) U-
687 series isotopes and destructive plate margin magma genesis in the Lesser Antilles. *Earth*
688 *and Planetary Science Letters*, 142, 191-207.
- 689 Valdes, M. C., Moreira, M., Foriel, J., & Moynier, F. (2014). The nature of Earth's building blocks
690 as revealed by calcium isotopes. *Earth and Planetary Science Letters*, 394, 135-145.
- 691 von Huene R. Shipboard Scientific Party (1982) Site 495: Cocos Plate – Middle America trench
692 outer slope. In: Aubouin J. et al. (eds) Initial Repots DSDP 67, 79-141.
- 693 Walter, M. J., Bulanova, G. P., Armstrong, L. S., Keshav, S., Blundy, J. D., Gudfinnsson, G., . . .
694 Gobbo, L. (2008). Primary carbonatite melt from deeply subducted oceanic crust. *Nature*,
695 464(622-625).
- 696 Wang, W., Zhou, C., Qin, T., Kang, J.-T., Huang, S., Wu, Z., & Huang, F. (2017). Effect of Ca
697 content on equilibrium Ca isotope fractionation between orthopyroxene and clinopyroxene.
698 *Geochimica et Cosmochimica Acta*, 219, 44-56.
- 699 Watkins, J. M., DePaolo, D. J., & Watson, E. B. (2017). Kinetic Fractionation of Non-Traditional
700 Stable Isotopes by Diffusion and Crystal Growth Reactions. *Reviews in Mineralogy and*
701 *Geochemistry*, 82, 85-125.
- 702 Wei, C.-W., Xu, C., Chakhmouradian, A.R., Brenna, M., Kynicky, J., Song, W.-L. (2020) Carbon-
703 Strontium Isotope Decoupling in Carbonatites from Caotan (Qinling, China): Implications
704 for the Origin of Calcite Carbonatite in Orogenic Settings. *Journal of Petrology*, ega024,
705 <https://doi.org/10.1093/petrology/egaa024>.
- 706 Wombacher, F., Eisenhauer, A., Heuser, A., & Weyer, S. (2009). Separation of Mg, Ca and Fe
707 from geological reference materials for stable isotope ratio analyses by MC-ICP-MS and
708 double-spike TIMS. *Journal of Analytical Atomic Spectrometry*, 24.
709 [doi:org/10.1039/b820154d](https://doi.org/10.1039/b820154d)
- 710 Zaitsev, A. N., & Keller, J. (2006). Mineralogical and chemical transformation of Oldoinyo Lengai
711 natrocarbonatites, Tanzania. *Lithos*, 91, 191-207.
- 712 Zhao, X., Zhang, Z. F., Huang, S., Liu, Y., Li, X., & Zhang, H. (2017). Coupled extremely light
713 Ca and Fe isotopes in peridotites. *Geochimica et Cosmochimica Acta*, 208, 368-380.
- 714 Zhu, P., & MacDougall, J. D. (1998). Calcium isotopes in the marine environment and the oceanic
715 calcium cycle. *Geochimica et Cosmochimica Acta*, 62, 1691-1698.
- 716
- 717

Table 1. Mass-dependent calcium isotope compositions of igneous rocks and standards.

Sample	Age (Ma)	$\delta^{44}\text{Ca}/^{40}\text{Ca}$	2σ	$\delta^{43}\text{Ca}/^{40}\text{Ca}$	2σ	n	Source
BSE							
Peridotite (avg)		0.01	0.04	-0.05	0.07	2	Simon and DePaolo (2010)
Peridotite (avg)		0.00	0.05	-	-	14	Kang et al. (2017)
Komatiite (avg)		-0.02	0.16	-	-	7	Amsellem et al. (2019)
Basalts							
BCR-1	15	-0.08	0.04	-0.05	0.07	2	Simon and DePaolo (2010)
BCR-2	15	-0.09	0.06	-	-	1	Simon et al. (2017)
OIB (avg)	1	0.00	0.04	-	-	7	Huang et al. (2010)
Koolau OIB (avg)	1	-0.15	0.06	-	-	6	Huang et al. (2011)
Mahukona OIB (avg)	1	-0.02	0.19	-	-	2	Huang et al. (2011)
Manua Kea OIB (avg)	1	-0.02	0.02	-	-	2	Huang et al. (2011)
BHVO-1 OIB	1	0.01	0.05	-	-	1	Huang et al. (2011)
BHVO-2 OIB	1	-0.05	0.05	-	-	1	Birmingham et al. (2018)
<i>average</i>		<i>-0.05</i>	<i>0.02</i>				
Arc Lavas							
AT-50		-0.08	0.14	-0.01	0.10	1	
YO1		-0.16	0.14	-0.18	0.11	1	
TE1		-0.12	0.14	-0.15	0.10	1	
SC2		0.06	0.05	0.07	0.05	4	Simon and DePaolo (2010)
<i>average</i>		<i>-0.07</i>	<i>0.05</i>	<i>-0.07</i>	<i>0.06</i>		
Carbonatites							
Laacher See 129	0.012900	-0.39	0.14	-0.27	0.25	1	
OL lava 2007	0.000013	-0.13	0.13	-0.06	0.10	2	
OL lava 4-7-08	0.000011	0.05	0.14	0.06	0.10	1	
Standards							
SRM915a		-0.95	0.04	-0.77	0.06	11	Simon and DePaolo (2010) = this study
Seawater (IAPSO)		0.81	0.16	-	-		Simon et al. (2017)
Seawater (GeoB 9506-4)		0.94	0.04	-	-	1	Birmingham et al. (2018)

*All reported where difference between BSE to SRM915a is 0.95 (Antonelli and Simon, 2020), cf. Simon and DePaolo (2010) saw an intrinsic effect in SRM915a, which leads to ~0.1 per mil increase in measured values reported relative to SRM915a (see text).

Table 2. Difference between igneous rocks used to estimate $\delta^{44}\text{Ca}/^{40}\text{Ca}$ of BSE and SRM915a standard for various laboratories.

Lab Facilities	Method	$\Delta^{44}\text{Ca}/^{40}\text{Ca}_{\text{BSE-SRM915a}}$	2σ	Source
Center for Isotope Geochemistry, University of California at Berkeley	DS-TIMS	0.97	0.07	Simon & DePaolo (2010); this work
Center for Isotope Cosmochemistry & Geochronology, NASA Johnson Space Center	DS-TIMS	0.96	0.04	Simon et al. (2017)
Isotope Research Geo- and Cosmochemistry Group, Harvard University	DS-TIMS	0.97	0.04	Huang et al. (2011)
State Key Laboratory of Isotope Geochemistry, Guangzhou Institute of Geochemistry, Chinese Academy of Sciences	DS-TIMS	0.94	0.04	Kang et al. (2017)
Institut für Mineralogie, WWU Münster*	DS-TIMS	0.91	0.03	Birmingham et al. (2018)
IFM-GEOMAR Leibniz-Institut für Meereswissenschaften, Keil, Germany & University of Saskatchewan Isotope Laboratory, Department of Geological Sciences, University of Saskatchewan, Canada	DS-TIMS	0.93	0.17	Amini et al. (2009)
Institut de Physique du Globe de Paris	MC-ICP-MS	0.90	0.08	Valdes et al. (2014)
Institut de Physique du Globe de Paris	MC-ICP-MS	1.00	0.10	Amsellem et al. (2019; 2020)
Princeton University**	MC-ICP-MS	0.99	0.14	Blattler & Higgins (2017)
Arizona State University**	DS-MC-ICP-MS	0.85	0.16	Ionov et al. (2019)
State Key Laboratory of Geological Processes and Mineral Resources, China University of Geosciences, Wuhan**	MC-ICP-MS	1.03	0.14	Chen et al. (2018; 2019a,b)

$$\Delta^{44}\text{Ca}/^{40}\text{Ca}_{\text{BSE-SRM915a}} = \delta^{44}\text{Ca}/^{40}\text{Ca}_{\text{BSE}} - \delta^{44}\text{Ca}/^{40}\text{Ca}_{\text{SRM915a}}$$

MC-ICP-MS methods obtain $\delta^{44}\text{Ca}/^{40}\text{Ca}$ by multiplying $\delta^{44}\text{Ca}/^{42}\text{Ca}$ by a scaling factor. If not stated standard errors are estimated by multiplying those reported by 2.049.

*Value estimated by comparison of reported $\delta^{44}\text{Ca}/^{40}\text{Ca}$ of BHVO-2 to that of Huang et al. (2011)

**Value estimated by comparison of reported $\delta^{44}\text{Ca}/^{40}\text{Ca}$ of SRM915b to that of Simon et al. (2017)

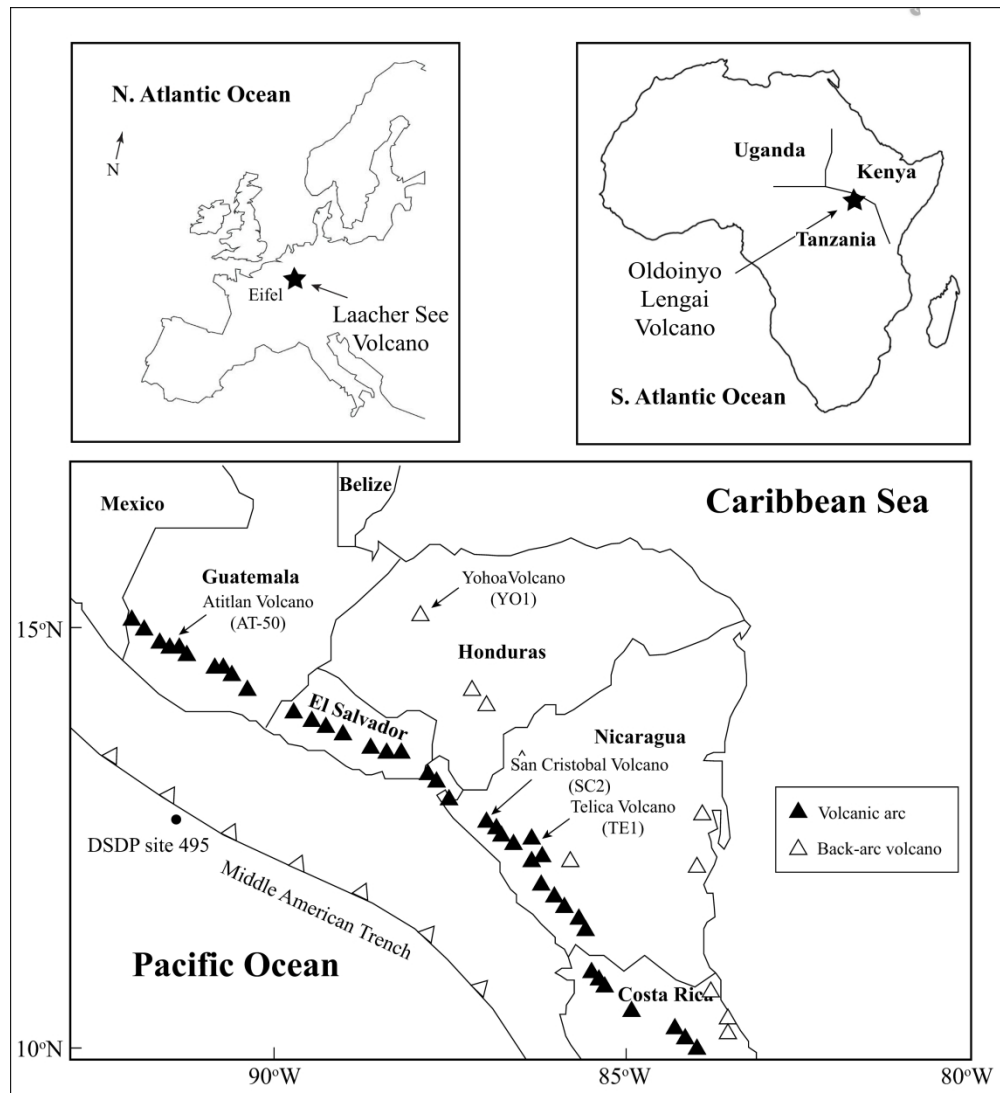


Figure 1. Maps of Central America, Eastern Africa, and Europe showing location of the studied samples. The location of the DSDP Site 495, off the coast of Guatemala, is also indicated (Central American map modified from Patino et al. 2000).

357x390mm (300 x 300 DPI)

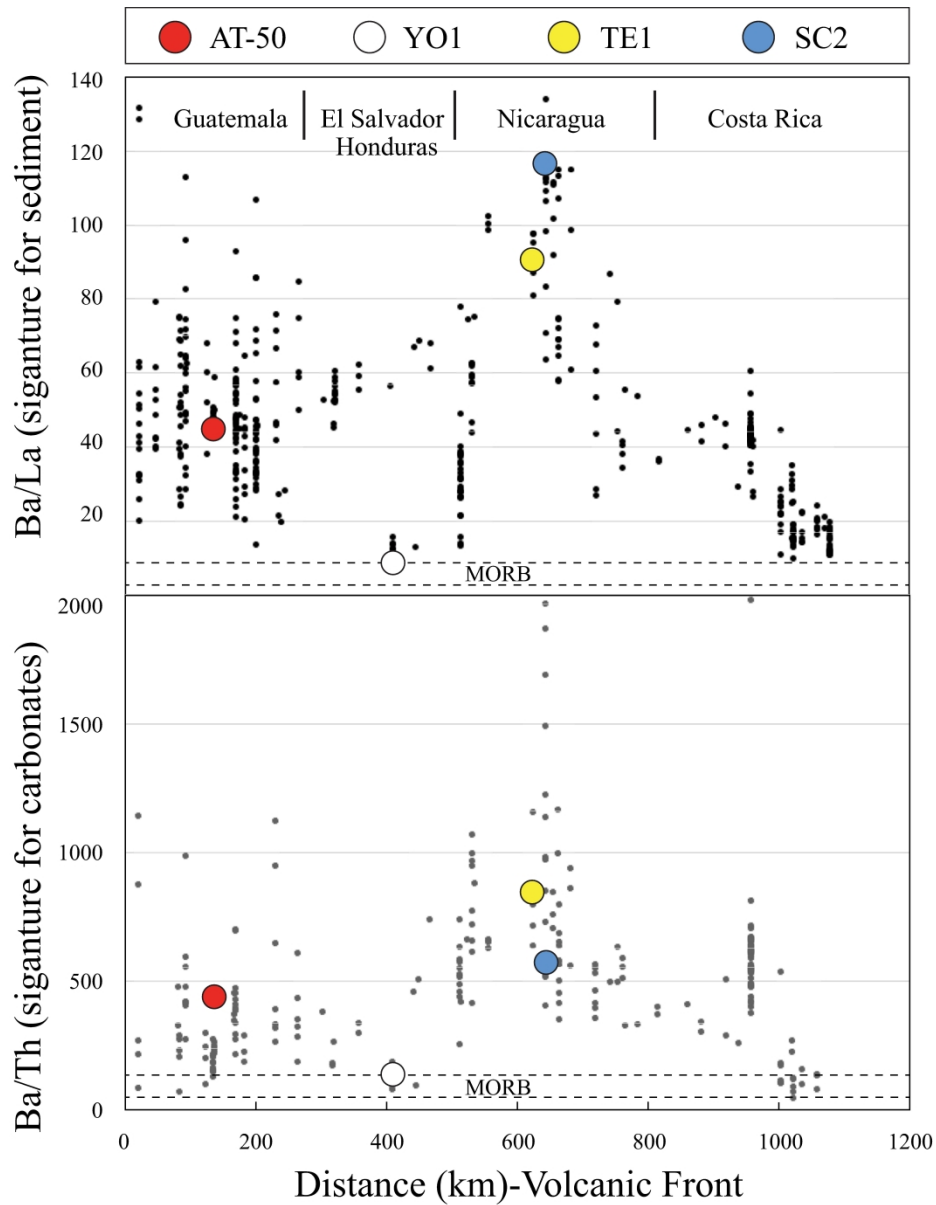


Figure 2. Regional variations in trace element ratios along the Central American volcanic arc. MORB-like Ba/La and Ba/Th values occur in Honduras volcanoes whereas maximum values, believed to be tracers of hemipelagic sediment and marine carbonate, respectively, occur in western Nicaraguan volcanoes (data from Patino et al., 1997; 2000).

259x336mm (600 x 600 DPI)

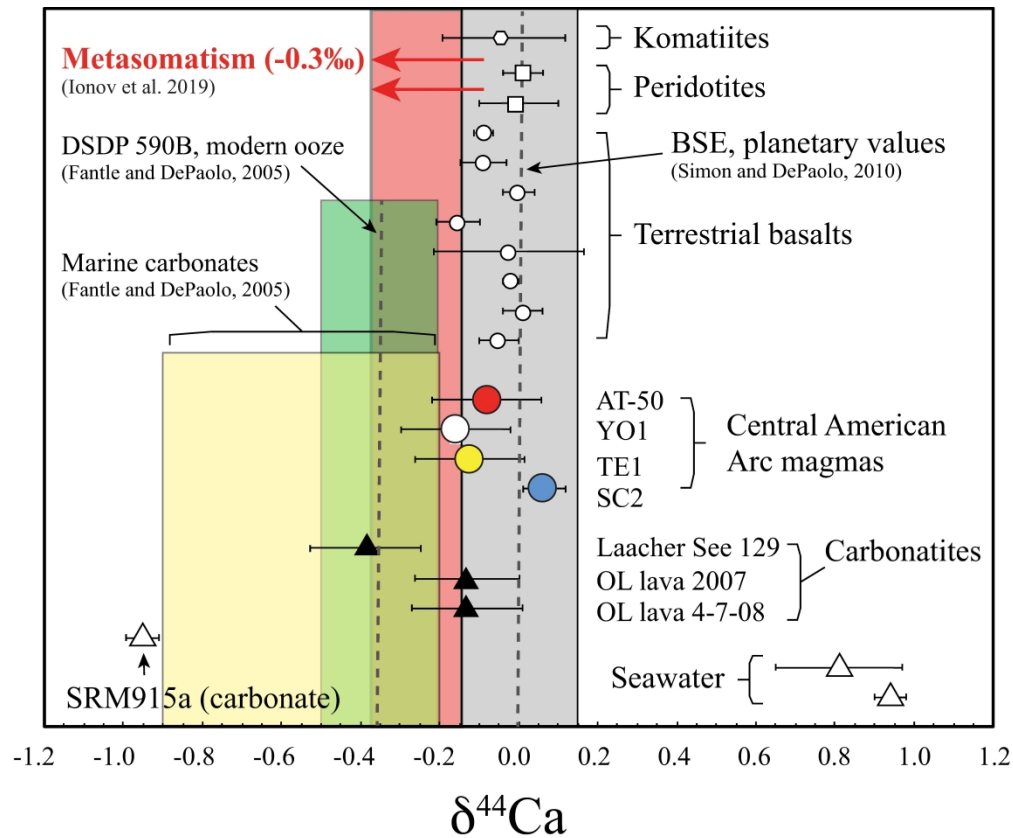
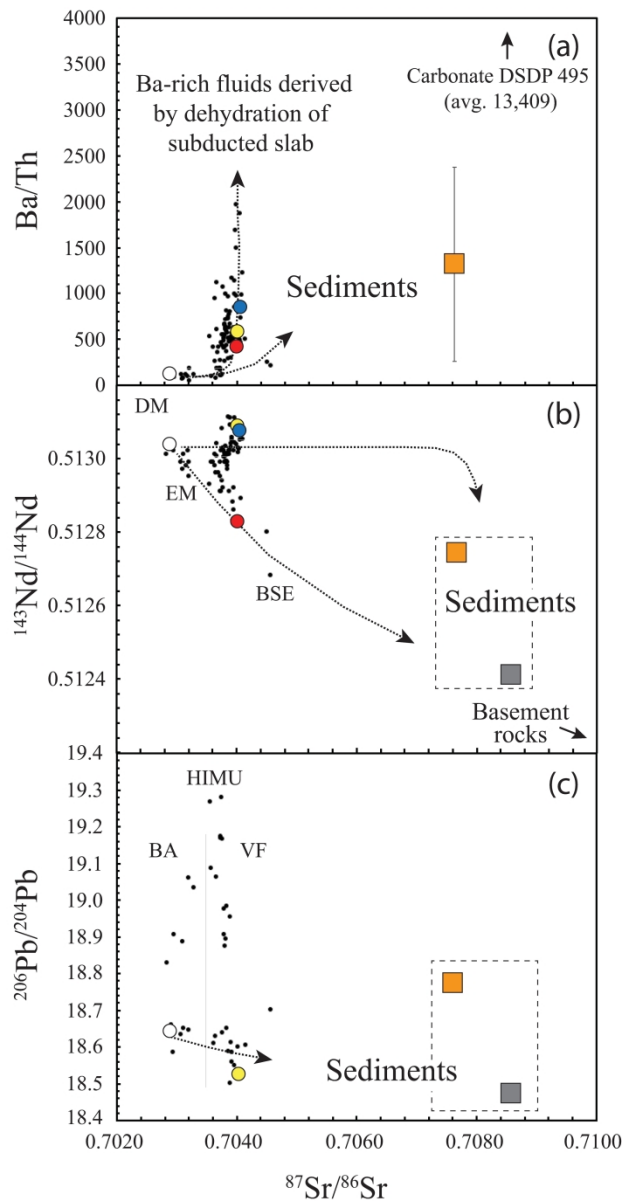


Figure 3. Calcium isotopic composition of Central American volcanic arc magmas (this study), extrusive Oldoinyo Lengai carbonatite lavas (this study), and intrusive Laacher See carbonatite clast (this study). Values for unmelted/unmetamorphosed peridotites, komatiites, terrestrial basalts, seawater, marine carbonates, SRM915a carbonate, and the effect of metasomatism shown for reference (Antonelli et al. 2019a; Amsellem et al., 2019; Bermingham et al., 2018; Fantle & DePaolo, 2005; Huang et al., 2010, 2011; Ionov et al., 2019; Kang et al., 2017; Simon & DePaolo, 2010; Simon et al., 2017). Not shown are the Precambrian carbonate data of Blattler and Higgins (2017) that exhibit an average $\delta^{44}\text{Ca}$ that is indistinguishable from BSE Ca isotope composition.

237x200mm (600 x 600 DPI)



Ba/Th- $^{87}\text{Sr}/^{86}\text{Sr}$ (a), $^{143}\text{Nd}/^{144}\text{Nd}$ - $^{87}\text{Sr}/^{86}\text{Sr}$ (b), and $^{206}\text{Pb}/^{204}\text{Pb}$ - $^{87}\text{Sr}/^{86}\text{Sr}$ (c) diagrams for Central American volcanic arc lavas. All samples from the volcanic front (VF) have geochemical signatures interpreted to be elevated above values for back-arc lavas (BA) by the addition of a sedimentary subducted component, e.g., enriched in $^{87}\text{Sr}/^{86}\text{Sr}$. Back-arc lavas including YO1 remain within the mantle field, reflecting mixtures of MORB-like depleted mantle and HIMU, enriched mantle (data and illustrative mixing curves from Carr et al., 1990; Feigenson & Carr, 1986; Feigenson et al., 2004; Patino et al. 1997; 2000). Orange and gray squares represent hemipelagic and carbonate DSDP 495 sediment compositions, respectively.

249x478mm (300 x 300 DPI)